Vehicle noise reduction of multiple load cases using vibro-acoustic potential analysis

F. Nentwich[1], T. Bartosch[1], G. Müller[1]

[1] MAGNA STEYR Fahrzeugtechnik, A-8041 Graz, Austria, Email: fred.nentwich@magnasteyr.com

Introduction

The engine and rolling noise are to be reduced with trim measures derived from a SEA model. Effective measures correspond to loss factors with high reduction potential. After setting up the model, there are some 25.400 non-zero coupling and internal loss factors to choose from; too much for manual labour. Therefore MAGNA STEYR developed the vibro-acoustic potential analysis [2]. It investigates how a loss factor variation affects the cabin's sound pressure level. The algorithm presumes realistic limits for the loss factor and calculates the maximum noise reduction that can be expected from practical measures. With this paper we show an extension of the VAPA in order to consider a multi-load case scenario. The VAPA identifies the most over all promising vibro-acoustic potentials. The engineer translates these into construction measures. Using this procedure a trim package originally weighing 12 kg is cut down to 6 kg, reducing both rolling and engine noise up to 1.5 dB(A).

Application

In a four wheel driven car a set of additional plattform trim measures is to be investigated with respect to engine noise [1] and rolling noise [6] [5] [8]. The complete set weighs 12 kg. It comprises heavy layers targeting floor transmission (fig.1) as well as fleeces targeting the rear fender cavity absorption. The most effective measures set are to be chosen to form a lighter subset [3] [7].

The model is set up in Auto-SEA. The panel structure stems from a FEM model. The model comprises 961 subsystems of which 3×293 are plates capable of extension waves, shear waves and flexure waves, 20 are interior cavities and 62 represent exterior cavities. Excluding the reciprocal CLFs there are 12.900 non-zero CLFs and ILFs together per frequency in $\mathbf{L}$. The excitations are measured on a prototype on a dynamometer test rig and then imposed on the model [3]. The structure-borne excitation subsystems comprise: the front axle carrier, the rear axle carrier, 4 engine carriers, the central drive train bearing, the rear cross beam, 4 rear longitudinal members and 4 strut towers. The air-borne excitation subsystems comprise: the engine bay, 4 wheelhouses and 4 underfloor cavities. Strictly speaking, the model is valid from 400 Hz to 6.3 kHz. But since observations in this model and other models display good agreement of simulation and measurement at even lower frequencies up to 200 Hz, the simulation is run at 200 Hz – 6.3 kHz.

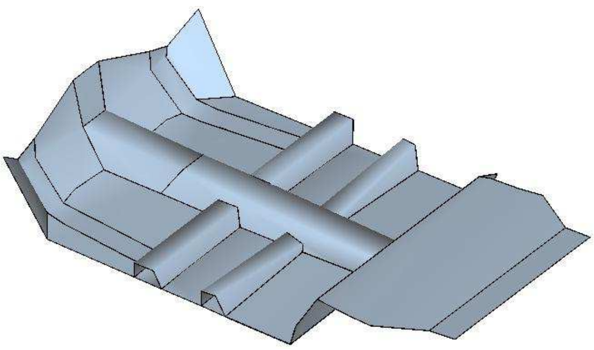

Figure 1: A heavy layer in the carpet abates sound transmission through the floor plates. The VAPA algorithm identifies where the heavy layer is most effective.

Vibro-acoustic Potential Analysis

SEA operates with the subsystem energy E_i, which can be transformed into a SPL for an air cavity, or into a vibration level for a steel plate. The energy balance [4] describes, how internal loss factors $\eta_{ii,(\omega)}$ and coupling loss factors $\eta_{ij,(\omega)}$ (both inside $\mathbf{L}$) translate the input power $P_{i,(\omega)}$ into the subsystem energy $E_{i,(\omega),(\underline{P})}$.

$$\omega \; \mathbf{L} \; \underline{E} \; = \; \underline{P} \qquad [\mathrm{W}] \qquad (1)$$

How does a variation of an arbitrary loss factor η_{ij} affect the driver's cabin's subsystem energy E_1? Using the reprocity therorem, [2] shows that the cabin's energy E_1 is a hyperbola function of the loss factor η_{ij}:

$$E_{1,ij,(\omega),(\underline{P})}(\eta_{ij}) \; = \; \frac{\eta_{ij} c_a + c_b}{\eta_{ij} + c_c}, \qquad [\mathrm{J}]$$
$$G_{1,ij}(\eta_{ij}) \; = \; \frac{\partial E_{1,ij}}{\partial \eta_{ij}} \; = \; \frac{c_a c_c - c_b}{(\eta_{ij} + c_c)^2} \qquad [\mathrm{J}] \qquad (2)$$

Eqn. (2) holds true for ILFs as well as CLFs. The angular frequency (w) as well as the load case $(\underline{P})$ are hereby frozen. The coefficients c_a, c_b, c_c are calculated by parameter variation [2]. The derivative $G_{1,ij}$ is the sensitivity of the cabin energy to the loss factor η_{ij}. Because $G_{1,ij}$ is either positive or negative $\forall \eta_{ij}$, $E_{1,ij}$ is monotonous and extrema are to be found on range boundaries or poles. The latter does not occur in reality. For CLFs an increase of coupling enlarges the subsystem's energy in most cases. Their sensitivities $G_{1,ij}$ are mostly positive, as shown in fig.2. For ILFs, an increase of damping lowers the energy of all subsystems. Their sensitivities $G_{1,ii}$ are negative.

The sensitivity $G_{1,ij}$ describes, how the receiver subsystem energy changes for *infinitesimal* variations of

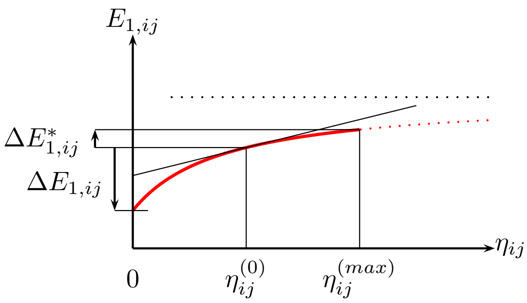

Figure 2: Receiver subsystem energy as a function $E_{1,ij}$ of the coupling loss factor η_{ij}. The actual vehicle design corresponds with $\eta_{ij}^{(0)}$. The vibro-acoustic potential $\Delta E_{1,ij}$ is the maximum reduction possible.

the loss factor η_{ij}. For practical applications, the maximum change achievable for realistic values of η_{ij} is of interest. This leads to the vibro-acoustic potential. It is the greatest theoretically possible reduction of receiver subsystem energy E_1 when η_{ij} is varied on a *global* scale while all other loss factors $\eta_{kl \neq ij}$ and the input powers P_k are kept constant. Hereby the angular frequency and the load case are kept frozen [2]. For CLFs, the range of η_{ij} is bounded by 0 and $\eta_{ij}^{(max)}$ which represent complete decoupling and strong coupling respectively. Often the lower boundary is of interest. For ILFs, η_{ii} is bounded by 0, corresponding to a totally reverberant subsystem, and $\eta_{ii}^{(max)}$. For air cavities $\eta_{ii}^{(max)}$ represents the theoretical case, where all cavity surfaces exhibit an absorption index of one thus violating SEA assumptions. For structure-borne sound $\eta_{ii}^{(max)}$ is represented when the steel plate has been completely covered with the thickest anti drumming pad imaginable [9]. Knowing the bounds of η_{ij} or η_{ii} and using (2), the minimum receiver subsystem energy possible can be calculated.

$$E_{1,ij,(\omega),(\underline{P}),\underline{min}} = \min\left\{ E_{1,ij}(0),\;\; E_{1,ij}(\eta_{ij}^{max})\right\}, [\mathrm{J}] \quad (3)$$

$E_{1,ij,(\omega),(\underline{P}),\underline{min}}$ is the vibro-acoustic potential for frozen angular frequency (ω) and load case $(\underline{P})$. The vibro-acoustic potential allows a judgement which loss factor would enable which reduction on a global scale of η_{ij}. Price, weight, feasibility in production and time-schedule tighten the realisable boundaries of η_{ij}. The vibro-acoustic potential tells us what can maximally be expected of a construction measure. Thus it enables the sorting of measures according to effectivity.

Multi Load Case Ranking

Loss factors with great vibro-acoustic potential are candidates for effective design modifications. Their vast number (here: 25.400) and various angular frequencies (ω) make the vibro-acoustic potential analysis necessary. However, the VAPA deals with only *one* load case $(\underline{P})$ at a time. A "conventional" loss factor ranking, for example, would be performed for rolling noise at 80 km/h. It would be practical, if the rolling noise ranking could simultaneously deal with several speeds, say 50, 80 and 100 km/h. Further, the ranking should comprise several load case types, such as rolling noise *and* engine noise. Thus the VAPA is extended by a multi load case ranking. One ranking strategy is, to collect measures important for each *single* load case. Since measures targeting rolling noise are added with measures targeting engine noise, this strategy might result in an expensive or heavy solution. A second ranking strategy is, that a measure should improve *all* examined load cases. This yields measures with a high cost and weight efficiency. Here the second strategy is persued. The multi load case VAPA has a four step procedure:

Step 1: For a fixed load case $\underline{P}$, the energy reduction $\Delta E_{1,ij,(\omega),(\underline{P})}$ is calculated for all ILFs and CLFs.

$$\begin{aligned} E_{1,(\omega),(\underline{P})} &= E_{1,ij,(\omega),(\underline{P})}(\eta_{ij}^{(0)}) \\ \Delta E_{1,ij,(\omega),(\underline{P})} &= E_{1,ij,(\omega),(\underline{P}),\underline{min}} - E_{1,(\omega),(\underline{P})}, [\mathrm{J}] \quad (4) \end{aligned}$$

Step 2: The maximum reduction $\Delta E_{1,ij,\underline{max},(\underline{P})}$ of each loss factor in the selected angular frequency range is acquired. This is repeated for each load case.

$$\Delta E_{1,ij,\underline{max},(\underline{P})} = \max_{(\omega)} \left\{ |\Delta E_{1,ij,(\omega),(\underline{P})}| \right\} \;\forall_{ij}, \forall_{(\underline{P})}$$

Step 3: These maxima are sorted for each load case: the highest maximum reduction is assigned the rank "1", the second highest the rank "2" and so on.

$$r_{1,ij,\underline{max},(\underline{P})} = \underset{ij}{\mathrm{sortindex}} \left\{ |\Delta E_{1,ij,\underline{\max},(\underline{P})}| \right\} \;\forall_{(\underline{P})}$$

Step 4: The rank of each loss factor η_{ij} or η_{ii} is averaged across all load cases $(\underline{P})$.

$$r_{1,ij,\underline{max},\underline{mean}} = \underset{(\underline{P})}{\mathrm{mean}} \left\{ r_{1,ij,\underline{\max},(\underline{P})} \right\},$$

The multi load case ranking provides the engineer with the 60 most important loss factors. The engineer makes the final selection, which loss factors are to be modified and seeks appropriate component measures. Generally, it is not possible to only change one single loss factor with a measure; several other loss factors will also be affected. The measures are therefore tested first in simulation and then on a prototype. Throughout the process the measures are discussed with departments involved to enforce a practical production.

In this application, the VAPA is performed in frequency range 250 Hz–2.5 kHz for the engine noise and the rolling noise. Three rankings, shown in table 1, are performed: "engine noise", "rolling noise" and "multi load". The loss factors, which cannot be influenced, have been removed from the table. The engine noise ranking was evalueated at 3000, 4000 and 5000 rpm. It yields that

Loss Factor		Ranking		
		EN	RN	Ml
cabin front absorption	(A)	1.	1.	1.
under floor cav.1 → cabin	(W)	3.	3.	2.
roof plate → cabin	(R)	4.	4.	3.
under floor cav.2 → cabin	(W)	8.	6.	4.
cabin rear absorption	(A)	14.	2.	5.
fire wall 6b → driver's cabin	(R)	5.	16.	6.
under floor cav.1 → floor 3a	(T)	7.	8.	7.
under floor cav.1 → floor 3b	(T)	17.	9.	8.
under floor cav.2 → floor 9b	(T)	20.	10.	9.
front door panel 1a → cabin	(R)	11.	12.	10.
front door panel 1b → cabin	(R)	12.	13.	11.
wheelhouse cav.→fender cav.	(W)	30.	5.	12.
under floor cav.2 → floor 9a	(T)	24.	14.	13.
floor plate 1a damping	(D)	19.	11.	14.
under floor cav.1 → floor 1a	(T)	28.	15.	15.
fire wall 6a → cabin	(R)	9.	16.	16.
engine bay cavity	(A)	2.	>100	>100
dashboard → cabin	(R)	10.	>100	>100
trunk cavity → cabin		>100	7.	>100

Table 1: Multi Load Ranking of CLFs and ILFs from absorption (A), structural damping (D), radiation (R), mass law (W) and transition from air born to structure-borne sound (T). A low rank number indicates a high importance. The engine noise ranking (EN) comprises 3000, 4000 & 5000 rpm. The rolling noise ranking (RN) comprises 50, 80 & 100 km/h. The multi load ranking (Ml) comprises both rolling and engine noise. It pinpoints loss factors important for both load cases.

the most important engine noise loss factors are the front cabin absorption, the engine bay absorption and the mass law from the underfloor cavity to the cabin. The rolling noise ranking was performed at 50, 80 and 120 km/h. Its most important loss factors are the front cabin absorption, the mass law from the underfloor cavity to the cabin and the rear cabin absorption. Note that the engine bay absorption does not show up in the rolling noise ranking. The multi load ranking identifies driver's cabin's absorption (rank 1 & 5), the mass law through the floor plates (rank 2 & 4) and the roof radiation (rank 3) as the crucial loss factors. Regarding the set of measures, the loss factors of the flat plates on the floor and firewall have the highest reduction potential. The tunnel and the crossbeams are less important (rank>100). With this a 6 kg set is conceptualized. In the simulation it has nearly the same reduction potential as the original 12 kg-trim, with *only* half the weight.

Simulation Result

The rolling noise simulation with and without extra trim is shown in fig.3 with the band-pass sound pressure level (BPSPL) from 250 Hz to 6.3 kHz as function of the vehicle speed. Without trim, the simulation's BPSPL (black, solid) is up to 3 dB(A) smaller than the measurement's BPSPL (black, dashed). The simulation of the 6 kg trim (blue) achieves nearly the same performance as the simulation of 12 kg trim (green). Their results differ by less than $\frac{1}{4}$ dB(A) BPSPL. This shows that the multi load case ranking, which led to the 6 kg subset, is highly effective. For both trims an average reduction of $1\frac{1}{2}$dB in BPSPL (250 Hz–6.3 kHz) at 50-120 km/h is achieved.

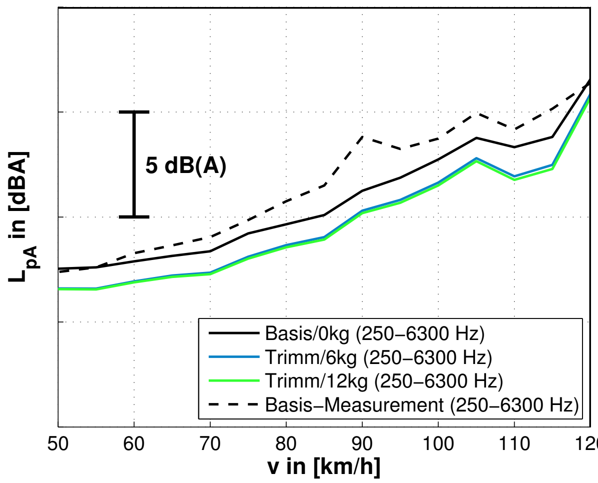

Figure 3: Rolling noise BPSPL simulation. The 6 kg trim (blue) achieves practically the same reduction as the 12 kg trim (green). The average reduction is $1\frac{1}{2}$dB in BPSPL.

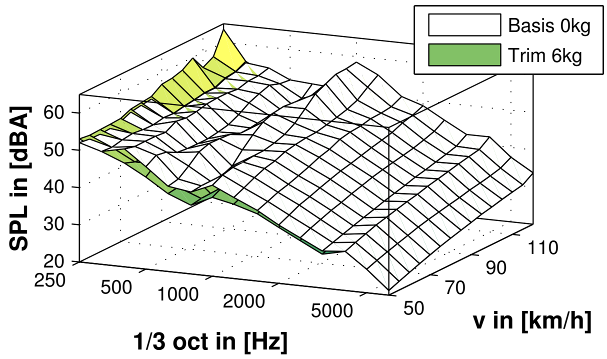

Figure 4: Rolling noise $1/3^{rd}$ octave band SPL as function of speed and frequency. The 6 kg-trim SPL (green) is lower than the 0 kg-basis SPL (white).

For rolling noise, fig.4 shows the $1/3^{rd}$ octave level as function of vehicle speed and frequency. The 6 kg trim SPL (green) lies below the 0 kg basis SPL (white) indicating reduction. Slight increases up to 1 dB(A) occur at 250 Hz. Small reductions of ≈ 1 dB(A) are found at 2-3 kHz. The largest reductions of up to 4 dB(A) are achieved at 400-1600 Hz.

The simulation of engine noise for 2000-6000 rpm shown in fig.5 with the BPSPL (200 Hz-6.3 kHz) as function of the rotational speed. Without trim, the simulation (black, solid) and the measurement (black, dashed) differ by 3 dB(A) BPSPL, or less. Again the effectiveness of the subset choise is demonstrated: the BPSPLs of the 6 kg trim (blue) and 12 kg trim (green) are almost the same. They differ by less than $\frac{1}{4}$ dB(A) BPSPL. For both trims achieve an average reduction of $1\frac{1}{2}$dB in BPSPL (250 Hz–6.3 kHz) at 2000-6000 rpm.

For engine noise, fig.6 shows the $1/3^{rd}$ octave level as function of the rotational speed and the frequency. By and large, the 6 kg trim SPL (green) lies below the 0 kg basis SPL (white) indicating noise reduction. Slight increases up to $1\frac{1}{2}$ dB(A) are found at 250 Hz and at 800 Hz. Large reductions of 3-$6\frac{1}{2}$ dB(A) are achieved at 400-500 Hz as well as at 1-5 kHz.

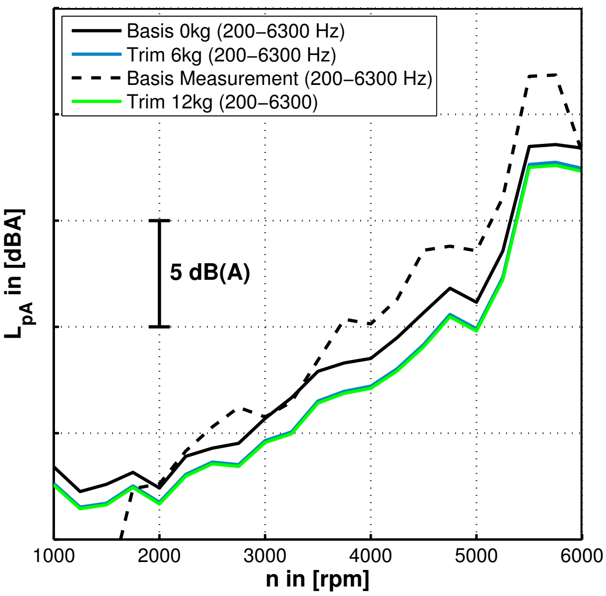

Figure 5: Engine noise BPSPL simulation. The 6 kg trim (blue) achieves practically the same reduction as the 12 kg trim (green). The average reduction is $1\frac{1}{2}$dB in BPSPL.

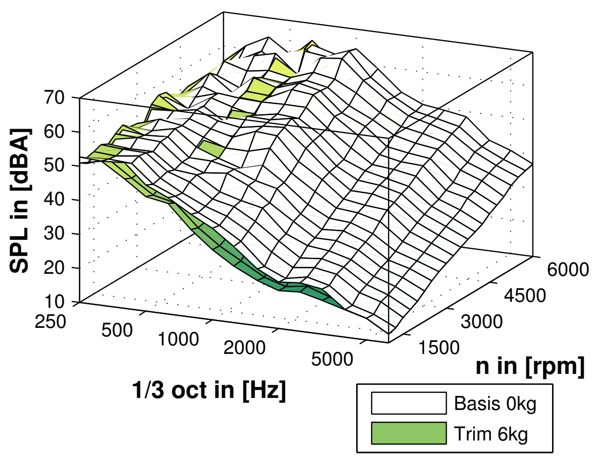

Figure 6: Engine noise $1/3^{rd}$ octave band SPL as function of speed and frequency at wide open throttle. The 6 kg-trim SPL (green) is lower than the 0 kg-basis SPL (white).

Synopsis

The vibro-acoustic potential analysis produces a ranking for *one* load case. By extending it with the multi load case ranking, loss factors important for *several* load cases can be identified. This is impressively demonstrated in an application example: starting from an original 12 kg trim set, the multi load case VAPA enables to conceptualize a 6 kg trim subset that reduces both rolling noise *and* engine noise to the same extent as the original trim set. The reduction is up to $1\frac{1}{2}$dB(A) in BPSPL (250 Hz–6,3 kHz) for both rolling and engine noise. The simulation's fine resolution enable to study changes beneath the measurement accuracy. With the vibro-acoustic potential analysis MAGNA STEYR has developed a powerful tool for the systematical choice of effective constructional measures.

References

[1] T. Bartosch, H. Macher, B. Kastreuz, C. Fankhauser: Optimize the acoustic concept using SEA vibro-acoustic potential analysis. In: *NVH Excellence - Achieving Results Beyond Customer Expectations*, p. 133-143, Graz, Austria, 15-17 Nov. 2006. ACC, AVL, MAGNA STERYR and SAE International.

[2] T. Bartosch, T. Eggner: Engine noise potential analysis for a trimed vehicle body: Optimisation using an analytical sea gradient computation technique. *JSV* **300** (1-2), 1-12, Feb. 2007.

[3] T. Bartosch, T. Eggner, K. Kolrus, H. Zach, and G. Müller. Simulationsgestützte Optimierung des Rollgeräusches im mittel- und hochfrequenten Bereich mit der Vibroakustischen Potenzialanalyse. In: *SIMVEC 2008,* VDI-Berichte 2031, Baden-Baden, Germany, November 2008. VDI.

[4] R. DeJong, R. H. Lyon: *Theory and Application of Statistical Energy Analysis*, Verl.: Butterworth-Heinemann, Newton/USA 1995.

[5] F. Nentwich: *Transfer-Pfad-Analyse im Zeitbereich zur Auralisierung von PKW-Innengeräuschen,* Shaker, Aachen, 2004.

[6] F. Nentwich, H. Finsterhölzl, H. Fastl: Darstellung und Beurteilung von Rollgeräusch-Anteilen, In: *Fortschritte der Akustik, DAGA 2002*, (DEGA Berlin), 208–209 (2002).

[7] F. Nentwich, Presentation of the Transfer Path Analysis of the Car's Interior Sound via Headphones, In: *Proc. of the 13th International Congress on Sound and Vibration* (ICSV13), Vienna, Austria, 2006.

[8] G. Müller, T. Bartosch, and T. Eggner. Optimisation of tyre noise transmission of a compact class vehicle using an experimental sea model. In *Proc. of EuroPAM user conference,* Toulouse, Frace, 10-12 October 2006. ESI Group.

[9] L. Wu, A. Agren: Analysis of initial decay rate in relation to estimates of loss factor and equivalent mass in experimental sea. In *Proc. of the International Conference on Noise & Vibration Engineering* (ISMA21), pages 187–198, Lulea University, Lulea, Sweden, September 1996. Acoustics Group.